

This is the accepted version of the following article:

Hadjidemetriou M., Papafilippou L., Unwin R.D., Rogan J., Clamp A., Kostarelos K.. Nano-scavengers for blood biomarker discovery in ovarian carcinoma. *Nano Today*, (2020). 34. 100901: - . 10.1016/j.nantod.2020.100901,

which has been published in final form at  
<https://dx.doi.org/10.1016/j.nantod.2020.100901> ©  
<https://dx.doi.org/10.1016/j.nantod.2020.100901>. This manuscript version is made available under the CC-BY-NC-ND 4.0 license <http://creativecommons.org/licenses/by-nc-nd/4.0/>

1  
2  
3  
4  
5  
6  
7  
8  
9  
10  
11  
12  
13  
14  
15  
16  
17  
18  
19  
20  
21  
22  
23  
24  
25  
26  
27  
28  
29  
30  
31  
32  
33  
34  
35  
36  
37  
38  
39  
40  
41  
42  
43  
44  
45

# **Nano-scavengers for Blood Biomarker Discovery in Ovarian Carcinoma**

Marilena Hadjidemetriou<sup>1\*</sup>, Lana Papafilippou<sup>1</sup>, Richard D. Unwin<sup>2</sup>, Jane Rogan<sup>3</sup>, Andrew Clamp<sup>4</sup> and Kostas Kostarelos<sup>1,5\*</sup>

<sup>1</sup>*Nanomedicine Lab, Faculty of Biology, Medicine & Health, AV Hill Building, The University of Manchester, Manchester, , United Kingdom*

<sup>2</sup>*Division of Cardiovascular Sciences, Faculty of Biology, Medicine & Health, The University of Manchester, Manchester, United Kingdom*

<sup>3</sup>*Manchester Cancer Research Centre Biobank, The Christie NHS Foundation Trust, CRUK Manchester Institute, Manchester, United Kingdom*

<sup>4</sup>*Institute of Cancer Sciences and The Christie NHS Foundation Trust, Manchester Cancer Research Centre (MCRC), The University of Manchester, Manchester, United Kingdom*

<sup>5</sup>*Catalan Institute of Nanoscience and Nanotechnology (ICN2), Campus UAB, Bellaterra, 08193 Barcelona, Spain*

---

\* Correspondence should be addressed to: [marilena.hadjidemetriou@manchester.ac.uk](mailto:marilena.hadjidemetriou@manchester.ac.uk)  
[kostas.kostarelos@manchester.ac.uk](mailto:kostas.kostarelos@manchester.ac.uk)

46 **Abstract**

47  
48  
49 The development and implementation of biomarker-based screening tools for ovarian cancer require  
50 novel analytical platforms to enable the discovery of biomarker panels that will overcome the  
51 limitations associated with the clinically used CA-125. The systematic discovery of protein  
52 biomarkers directly from human plasma using proteomics remains extremely challenging, due to the  
53 wide concentration range of plasma proteins. Here, we describe the use of lipid-based nanoparticles  
54 (NPs) as an 'omics' enrichment tool to amplify cancer signals in the blood and to uncover disease  
55 specific signatures. We aimed to exploit the spontaneous interaction of clinically-used liposomes  
56 (Caelyx®) with plasma proteins, also known as 'protein corona' formation, in order to facilitate the  
57 discovery of previously unreported differentially abundant molecules. Caelyx® liposomes were  
58 incubated with plasma samples obtained from advanced ovarian carcinoma patients and healthy  
59 donors and corona-coated liposomes were subsequently recovered. Comprehensive comparison  
60 between 'healthy' and 'diseased' corona samples by label-free proteomics resulted in the  
61 identification of multiple differentially abundant proteins. Moreover, immunoassay-based validation  
62 of selected proteins demonstrated the potential of nanoparticle-platform proposed to discover novel  
63 molecules with great diagnostic potential. This study proposes a nanoparticle-enabled workflow for  
64 plasma proteomic analysis in healthy and diseased states and paves the way for further work  
65 needed to discover and validate panels of novel biomarkers for disease diagnosis and monitoring.

66  
67  
68 **Keywords:** protein corona, biomarkers, ovarian cancer, liposomes, nanomedicine

69  
70  
71  
72  
73  
74  
75  
76  
77  
78  
79  
80  
81  
82  
83  
84  
85  
86  
87  
88  
89  
90  
91

## 92 Introduction

93

94 Much effort is currently focused on the development of robust and high-throughput ‘omics’  
95 platforms for the discovery of minimally invasive molecular biomarkers to aid early and accurate  
96 cancer diagnosis, monitor tumour growth and response to therapies. Despite significant investment  
97 by major stakeholders, few protein cancer biomarkers have been validated and received FDA  
98 approval, raising concerns regarding the efficiency of the biomarker-development pipeline. It is  
99 noteworthy that of the FDA-approved biomarkers, the majority are used to monitor the progression  
100 of cancer, rather than enabling its early diagnosis.<sup>1</sup>

101 Proteins are the biological endpoints that govern most pathophysiological processes and  
102 they have therefore attracted most interest so far as biomarkers for cancer diagnostics.<sup>2</sup> Blood is  
103 frequently the biosample of choice for biomarker identification; however the discovery of tumour-  
104 derived protein signatures directly from blood is hindered by the wide concentration range of blood  
105 proteins, in addition to the preponderance of highly abundant proteins.<sup>3</sup> Despite significant  
106 improvement in the sensitivity of mass spectrometry-based proteomics, the issue of the high  
107 dynamic range of plasma protein abundances still remains unresolved and the diagnostic  
108 information blood can offer is partially inaccessible.<sup>4</sup>

109 Nanotechnology-based platforms hold great promise in addressing the above issues  
110 associated with biomarker discovery.<sup>5</sup> It should be emphasised however, that the vast majority of  
111 nanoparticle-based technologies developed so far have been designed to capture and quantify  
112 already known cancer-specific analytes,<sup>6-9</sup> enabling the verification and validation phases of  
113 biomarker development. The NP-enabled discovery of new plasma buried biomarkers has only  
114 been recently attempted.<sup>10</sup>

115 The fact that the surface of NPs is instantly covered by a wide range of adsorbed proteins  
116 and other biomolecules once in contact with blood, a self-assembly phenomenon known as  
117 ‘protein’ or ‘biomolecule’ corona formation,<sup>11,12</sup> makes NPs ideal biomarker discovery platforms.  
118 Biomolecule corona formation has become a popular line of research in the last decade and  
119 ongoing research is mainly focused on the proteomic analysis of corona profiles after the *ex vivo*  
120 and more recently the *in vivo* interaction of NPs with biofluids (mainly plasma).<sup>13-17</sup> Nanoparticle-  
121 protein interactions at the bio-nano interface not only can shed new light on the development of  
122 nanotechnologies but are now gradually being exploited as an engineering tool with therapeutic  
123 and diagnostic capabilities.<sup>10,11,18-20</sup>

124 The surface-capture of a complex blood proteome by NPs as well as the recently proposed  
125 concept of ‘personalized corona’ has sparked interest for utilizing the biomolecule corona

126 fingerprinting as a proteomic discovery platform.<sup>10,18,21,22</sup> We have recently demonstrated that the  
127 NP protein corona formed in the blood circulation of humans has the potential to be exploited as an  
128 enrichment and pre-fractionation tool that allows in depth coverage of the plasma proteome.<sup>18</sup> In a  
129 subsequent study, we employed two different tumour mouse models (a subcutaneous melanoma  
130 model and human lung carcinoma xenograft model) to demonstrate that intravenously injected  
131 lipid-based NP-scavengers (liposomes) surface-capture low MW, low abundant and disease-  
132 specific plasma proteins which cannot be detected by conventional plasma proteomic analysis.<sup>10</sup>  
133 Moreover, this study demonstrated that protein coronas, formed around intravenously injected  
134 NPs, differ both quantitatively and qualitatively in the presence and absence of a disease, allowing  
135 the uncovering of differentially abundant potential biomarker proteins.<sup>10</sup>

136 When animal models are employed for biomarkers discovery the exploitation of the  
137 molecularly richer *in vivo* protein corona is advantageous as opposed to its counterpart *ex vivo*  
138 corona.<sup>16</sup> However, hypothesis-free discovery proteomics often require the use of human clinical  
139 samples and therefore, in this study we aimed to explore the use of the *ex vivo* protein corona  
140 formed around the clinically used PEGylated liposomal doxorubicin formulation (Caelyx®), to  
141 identify disease-specific proteins directly from plasma samples, obtained from patients with  
142 recurrent ovarian carcinoma.

143 The work flow of this study is summarized in **Figure 1A** and involved the incubation of  
144 Caelyx® liposomes with plasma samples from patients with recurrent ovarian cancer and from  
145 healthy donors and the comprehensive comparison of the resultant protein coronas by label-free  
146 mass spectrometry. The above analysis led to in the discovery of 413 differentially abundant  
147 proteins between 'healthy' and 'diseased' corona samples, of which nine were quantified by  
148 immunoassays to further validate the potential use of the nanoparticle-protein corona technology  
149 for plasma proteomic analysis and biomarkers discovery.

150  
151  
152  
153  
154  
155  
156  
157  
158  
159  
160  
161  
162

## 163 **Results**

164  
165 **Recovery and purification of corona-coated liposomes from plasma samples obtained from**  
166 **ovarian carcinoma patients and healthy donors.** To investigate the exploitation of the *ex vivo*  
167 formed NP protein corona for biomarker discovery, Caelyx® liposomes (20 µl of 1.5mM) were  
168 incubated with plasma samples (980 µl) obtained from patients with recurrent ovarian carcinoma  
169 about to commence the first cycle of Caelyx® as part of standard-of-care treatment (n=19) and  
170 age- matched female healthy donors (n=10). Patient clinical and basic blood analysis  
171 characteristics are summarized in **Tables S1** and **S2**. The physicochemical characteristics of the  
172 Caelyx® liposomes employed are summarized in **Table S3**. It should be noted that Caelyx® was  
173 employed because of its clinical use for the treatment of advanced ovarian cancer. The presence  
174 of the encapsulated doxorubicin has been shown not to affect the surface properties of liposomes  
175 and therefore corona formation.<sup>15</sup>

176 The *ex vivo* protein corona was allowed to form upon incubation of Caelyx® liposomes with  
177 plasma samples for 90 min at 37°C (**Figure 1A**). A purification protocol dependent on size  
178 exclusion chromatography was immediately performed to separate corona-coated liposomes from  
179 unbound plasma proteins. Membrane ultrafiltration was then used to concentrate the corona  
180 samples and to remove any large unbound or softly attached proteins, as previously optimised and  
181 described.<sup>10,13-16,18</sup> The above two-step purification process results in the complete elimination of  
182 unbound plasma proteins as demonstrated by plasma control experiments (**Figure S1**).

183 To confirm corona formation and to assess the morphology of Caelyx® liposomes before  
184 and after corona formation, Transmission Electron Microscopy (TEM) was performed. A well-  
185 dispersed liposome suspension was observed before and after incubation with plasma samples  
186 and purification. Corona-coated Caelyx® liposomes retained their size and spherical structure,  
187 while the occurrence of the proteins attached onto their surface revealed protein corona formation  
188 (**Figure 1B**).

189 To quantitatively compare 'healthy' and 'diseased' protein coronas, we calculated the total  
190 amount of protein associated with each µmole of lipid (Protein binding value; Pb). As shown in  
191 **Figure 1C**, the average Pb value for ovarian carcinoma patients was 4 times higher than the  
192 average Pb value observed for healthy controls. These results are in agreement with our previous  
193 investigations in preclinical mouse models showing that protein corona fingerprints quantitatively  
194 differ in the absence and presence of tumorigenesis.<sup>10</sup>

195 Proteins associated with Caelyx® liposomes were separated by SDS-PAGE and visualized  
196 by Imperial Protein stain, as illustrated in **Figure 1D**. Despite the higher total amount of protein  
197 observed in the 'diseased' coronas, well distinct protein bands even at the low MW region were

198 observed, demonstrating the ability of the NP enrichment platform technology to minimise the noise  
199 of highly abundant proteins, such as albumin, and allow the interaction with low abundant proteins.  
200 The extensive purification processes applied to retrieve the corona-coated liposomes and purify  
201 them from the unbound proteins, worked as fractionation tool allowing the uncovering of the low  
202 MW plasma proteome (**Figure 1D**).

203 **Proteomic comparison of ‘healthy’ and ‘diseased’ protein coronas.** The goal of the  
204 proteomic discovery experiment was to comprehensively compare the ‘healthy’ and ‘diseased’  
205 coronas in order to identify differentially abundant proteins.

206 In order to assess the reproducibility of the analysis of protein corona by LC-MS/MS, we  
207 isolated corona-coated liposomes from 6 aliquots of the same plasma sample (obtained from one  
208 healthy donor). The results demonstrated that the purification and quantification of the  
209 nanoparticle-bound protein fraction was reproducible, with 73% of proteins being measured with  
210 <30% CV (**Figure S2A**). To further validate the experimental reproducibility, two of the above  
211 replicated samples were analyzed in triplicates to evaluate the repeatability of the LC:MS/MS  
212 platform and the results demonstrated high analytical precision with approximately 95% of  
213 identified proteins with <30% CV (**Figure S2B & S3**). To assess the linearity of protein adsorption  
214 we incubated the same concentration of Caelyx® liposomes in full and diluted plasma.  
215 Interestingly, the total amount of corona proteins adsorbed onto the surface of liposomes was  
216 directly proportional to the total protein concentration in the incubation medium (**Figure S4**).

217 To compare ‘healthy’ and ‘diseased’ coronas, equal amounts of total protein from each  
218 corona sample were digested and subsequently analysed by LC-MS/MS. It should be emphasized  
219 that albumin and immunoglobulins were not depleted from corona samples prior to proteomic  
220 analysis. Processing of the raw data generated by LC-MS/MS analysis with Progenesis Q1 (version  
221 3.0; Nonlinear Dynamics) software tool was carried out to statistically compare the abundance of  
222 proteins present in the ‘healthy’ and ‘diseased’ liposomal coronas. The Relative Protein Expression  
223 (fold change) and the reliability of measured differences (ANOVA, *p value*) were calculated.

224 **Figures 2A & 2B** highlight the subset of differentially abundant proteins that met our confirmation  
225 criteria (see Experimental Section for further details). Out of 1187 identified proteins, 413 were  
226 found to be differentially abundant between the two groups with a *p value* <0.05, of which 171 were  
227 upregulated and 242 downregulated (**Figure 2B & Table S4**). Considering the importance of  
228 achieving high confidence in the discovered proteins, we applied even more stringent criteria and  
229 interestingly out of the above 413 differentially abundant proteins 303 had a *p value*<0.01 (FDR of  
230 2%) and a fold change > 2, which represents 25.5% of all proteins identified (**Figure 2B**).

231 The majority of highly specific cancer biomarkers are low MW intracellular proteins released  
232 from the tumour microenvironment into the blood circulation by leakage or secretion, however, their  
233 detection by plasma proteomic analysis remains challenging due to their extremely low  
234 concentration in the ng/ml to pg/ml range.<sup>23</sup> Interestingly, classification of the differentially abundant  
235 proteins identified in this study according to their cellular localization, demonstrated the enrichment  
236 of 189 intracellular proteins (present in the cytoplasm or nucleus) onto the surface of liposomes  
237 (**Figure S5**). In addition, ~50% of the differentially abundant proteins discovered had a MW < 60  
238 kDa (**Figure S6**).

239 The above observation prompted us to investigate whether the differentially abundant  
240 corona proteins have been previously associated with ovarian carcinoma pathways. Disease and  
241 function IPA search revealed the association of 335 and 60 corona proteins with solid tumour  
242 pathways and metastasis processes, respectively. Interestingly, 72 proteins have been previously  
243 associated with ovarian cancer pathways, of which 15 have been described in the literature as  
244 potential biomarkers for ovarian cancer (n=8 for diagnosis; n=5 for unspecified applicability, n=1 for  
245 safety; and n=2 for efficacy), (**Figure 3**).

246 The plasma-incubated liposomes also surface-captured the clinically used blood biomarkers  
247 CA 125 (MUC 16), Transthyretin (TTR) and Apolipoprotein A1 (APOA1), all included in the FDA  
248 approved OVA1 diagnostic test which is used to evaluate ovarian masses for cancer prior to  
249 planned surgery.<sup>24</sup> In agreement with OVA1 test, CA125 and B2M were found to be upregulated in  
250 the 'diseased' corona whereas APOA1 was found to be downregulated. This suggests that the  
251 abundance of corona proteins, as calculated by LC-MS/MS analysis, directly reflects their  
252 concentration in blood.

253 Overall, the above data suggest that analysis of protein coronas formed after the *ex vivo*  
254 incubation of liposomes with plasma samples obtained from cancer patients and healthy controls  
255 can be used to uncover differentially abundant proteins, otherwise buried under the overwhelming  
256 signal of albumin.

257  
258 **Validation of the nanoparticle protein corona technology.** To verify that the level of fold change  
259 observed by proteomic analysis of the 'healthy' and 'diseased' coronas is representative of the  
260 plasma proteome in healthy and diseased states, we performed ELISA experiments using plasma  
261 samples obtained from the same ovarian carcinoma patients and healthy controls. Distribution of  
262 the differentially abundant proteins identified by statistical significance and magnitude of change  
263 revealed that the majority exhibited fold change values much higher than the clinically used  
264 biomarkers CA125, TTR, and APOA1 (**Figure 2B & 4A**).



265           Nine corona proteins were selected to be validated and were divided in three groups: a)  
266 clinically used biomarkers for ovarian cancer (CA125, APOA1 and TTR; shown in orange); b)  
267 proteins mapped by IPA software to be associated with ovarian carcinoma pathways (THBS1,  
268 ENO1 and TGF- $\beta$ 1; shown in green) and c) proteins that have not been previously associated with  
269 ovarian carcinoma pathways but exhibited very promising fold change and *p values* (NME1, PDIA4  
270 and PRKCSH; shown in blue). The fold change and *p values* of the nine selected proteins (as  
271 calculated by LC-MS/MS analysis) are illustrated in (**Figures 4A & S7**).

272           The plasma concentration profiles of selected proteins and their respective ROC curves, as  
273 calculated by ELISA experiments are shown in **Figure 4B**. In agreement with LC-MS/MS data  
274 (**Figures 4A & S7**), APOA1 and TTR proteins were found to be downregulated while CA125,  
275 THBS1, ENO1, TGF- $\beta$ 1, NME1, PDIA4 and PRKCSH proteins were found to be upregulated in  
276 ovarian carcinoma patients (**Figure 4B**). This indicates that changes in the plasma proteome are  
277 directly reflected in the protein corona composition.

278           As illustrated in **Figure 4B**, the second group of proteins showed greater specificity and  
279 sensitivity than the clinically used biomarkers with AUC values ranging between 97.6% and 99.4%.  
280 Strikingly, an AUC value of 100% was observed for PDIA4 and PRKCSH proteins. The above  
281 ELISA validation data provide the first experimental evidence that *ex vivo* corona proteomic  
282 profiling provides allows increased penetration into the plasma proteome and has the potential to  
283 allow the discovery of candidate biomarkers.

284

## 285 **Discussion**

286

287           In the UK, 55-58% of ovarian carcinoma patients are diagnosed at stage III or IV and 42-  
288 45% are diagnosed at stage I or II. Survival for ovarian cancer is strongly related to the stage of the  
289 disease at diagnosis (99% of patients diagnosed at stage I survive their disease for at least one  
290 year, versus 51% of patients diagnosed at stage IV).<sup>25</sup> The lack of disease-specific symptoms, in  
291 addition to the limited performance of the clinically used CA-125 serum biomarker, indicates the  
292 need for new biomarker-based tools to accurately detect ovarian cancer and to monitor disease  
293 progression.<sup>26</sup>

294

295           Label-free proteomics profiling of blood is a powerful tool to detect molecular biomarkers that  
296 are differentially expressed between healthy and disease states.<sup>27</sup> The concentration of a complex  
297 network of proteins that regulate tumorigenic pathways is often altered in the blood circulation of  
298 cancer patients; however their identification is hampered by the wide dynamic range of plasma  
proteins. Due to the limited analytical sensitivity, currently available mass spectrometry-based

299 approaches predominantly detect highly abundant proteins of limited diagnostic use and fail to detect  
300 low MW tumour-tissue derived proteins of lower abundance. To overcome the issue of albumin  
301 masking, plasma immunodepletion columns are extensively employed, however their use is limited  
302 by a significant loss of low MW proteins along with the highly abundant carrier plasma proteins.  
303 Therefore, the multifaceted process of tumorigenesis necessitates the development of 'omics-  
304 enrichment' platforms that will enable the discovery of biomarker panels with sufficient specificity and  
305 sensitivity.

306 We have recently proposed the use of nanoparticles (NPs) as protein-scavenging  
307 enrichment platforms to address the above fundamental issues associated with biomarker  
308 discovery in plasma. Our results demonstrated that intravenously administered lipid-based NPs, in  
309 mice and humans, were able to surface-capture and amplify low abundant tumour-released  
310 molecules that could not be detected by conventional plasma proteomics analysis.<sup>10,18</sup> This idea of  
311 using nanoparticles to allow an in depth-analysis of the blood proteome is based on the  
312 spontaneous and non-targeted adsorption of hundreds of proteins onto the nanoparticles surface  
313 once in contact with biological fluids, a phenomenon known as 'protein corona' formation.<sup>11</sup>

314 Herein, we aimed to further explore and validate the potential use of the nanoparticle-protein  
315 corona to discover novel disease-specific proteins from plasma samples obtained from ovarian  
316 carcinoma patients (**Figure 1A and Tables S1 & S2**). Even though analysis of the *in vivo* formed  
317 protein corona (after intravenous administration of NPs) has been shown to result in a richer sampling  
318 of the blood proteome,<sup>16</sup> exploitation of the *ex vivo* protein corona (after incubation of NPs with  
319 plasma samples) could be more easily incorporated in the discovery phase of the biomarker pipeline  
320 and deserves further investigation. It should be emphasized that unlike other nanoparticle-based  
321 technologies aiming to increase the sensitivity of detection of already known molecules,<sup>8,28</sup> the  
322 technology platform proposed here aims to identify previously unseen potential biomarker proteins  
323 that could potentially offer higher specificity and sensitivity than the clinically used biomarkers.

324 To assess the potential of the NP protein corona technology as a tool for biomarker  
325 discovery, we comprehensively compared protein coronas formed around a clinically used  
326 liposomal formulation, Caelyx®, upon incubation with plasma samples obtained from healthy  
327 donors (n=10) and from patients with recurrent ovarian cancer (n=19). Immediately after plasma  
328 incubations, corona-coated liposomes were purified from any unbound plasma proteins and only  
329 liposome-bound proteins were analysed by LC-MS/MS. It should be emphasized that albumin and  
330 immunoglobulins were not depleted from corona samples prior to LC-MS/MS analysis. Even  
331 though a fraction of highly abundant proteins interacts with the surface of liposomes, any unbound  
332 highly abundant proteins are removed by the purification process which addresses the 'signal-to-

333 noise' issue that biomarker discovery suffers from. We therefore propose that analysis of the  
334 nanoparticle protein corona can substitute plasma fractionation and immunodepletion  
335 methodologies.

336 In agreement with our previous studies in tumour-bearing mice,<sup>10</sup> we observed a  
337 significantly higher total amount of protein adhered onto the NPs surface in ovarian carcinoma  
338 patients in comparison to healthy controls (**Figure 1C**). This observation, not only confirms our  
339 hypothesis that protein corona is greatly affected by the ongoing tumorigenesis but it also paves  
340 the way for the development of diagnostic tests. More studies are needed to assess if the  
341 fluctuation in the amount of protein adsorbed onto the NPs surface can be used to indicate the  
342 onset of a disease or to monitor disease progression and response to the treatment.

343 Despite the higher amount of protein adhered onto the NPs surface after incubation with  
344 plasma samples obtained from ovarian carcinoma patients, gel electrophoresis experiments  
345 indicated that the analysis of the NP protein corona eliminates the issue of albumin masking and  
346 enables the analysis of a broad range of the plasma proteins including low MW proteins (**Figure**  
347 **1D & Figure S5**). Subsequent analysis of the NPs protein coronas by LC-MS/MS revealed 413  
348 proteins that were differentially abundant between ovarian carcinoma patients and healthy controls  
349 (with a *p value* < 0.05), of which 171 were under-expressed and 242 over-expressed (**Figures 2A**  
350 **& B**). Recent ongoing biomarker development efforts indicate that multiple markers, used  
351 individually or as part of a panel, are required to provide sufficient sensitivity and specificity.  
352 Noteworthy, although the majority of proposed cancer biomarkers are proteins found to be  
353 upregulated in the blood circulation of cancer patients, downregulated biomarkers are currently  
354 clinically used and should be taken into consideration.<sup>26</sup>

355 According to Ingenuity Pathway Analysis, out of 413 differentially abundant proteins  
356 discovered in this study 57 have been previously associated with ovarian carcinoma pathways and  
357 only 15 have been previously proposed as potential biomarkers for ovarian cancer (**Figure 3**).  
358 Moreover, distribution of the differentially abundant proteins identified by statistical significance and  
359 magnitude of change (**Figure 2B**) revealed that n=303 proteins had a *p value*<0.01 and a fold  
360 change> 2. It should be noted that even though the clinically used biomarkers CA125, TTR and  
361 APOA1 were found to interact with the surface of liposomes, the majority of differentially abundant  
362 proteins identified, exhibited higher fold change values with higher statistical significance in  
363 comparison to the clinically used biomarkers (**Figure 3B**). These results suggest that analysis of  
364 the NP protein corona can unveil previously unseen disease-specific molecules, otherwise buried  
365 under the overwhelming signal of albumin and immunoglobulins. More studies are needed to prove  
366 the ability of this nanoplatform to enrich disease-specific molecules at the early asymptomatic

367 stages of cancer. Moreover, pathway analysis of the 'diseased' nanoparticle corona could provide  
368 valuable information about the ongoing pathological pathways and the mechanism of cancer  
369 initiation and progression and could potentially lead to discovery of novel therapeutic strategies.

370 The identification of previously unknown disease-specific proteins prompted us to verify the  
371 differences observed between 'healthy' and 'diseased' coronas by commercially available ELISA  
372 kits, using plasma samples obtained from the same ovarian carcinoma patients and healthy  
373 controls. We chose to validate and compare 3 groups of proteins: a) clinically used biomarkers for  
374 ovarian cancer (CA125, APOA1 and TTR), b) proteins mapped by IPA software to be associated  
375 with ovarian carcinoma pathways (THBS1, ENO1 and TGF- $\beta$ 1) and c) proteins that have not been  
376 previously associated with ovarian carcinoma pathways (NME1, PDIA4 and PRKCSH). ELISA data  
377 were found to directly reflect the changes observed by LC-MS/MS analysis of 'healthy' and  
378 'diseased' corona samples (**Figure 4**), indicating that protein corona composition mirrors the  
379 concentration fluctuations of the plasma proteome in the presence of a disease. Interestingly,  
380 ELISA quantification of the last two groups of proteins revealed higher performance than the  
381 clinically used biomarkers with AUC values between 97.6% and 99.4%, while an AUC value of  
382 100% was shown for PDIA4 and PRKCSH proteins. Given the same plasma source was used for  
383 the corona formation and ELISA experiments, the above data represent solely an orthogonal  
384 validation of the LC-MS/MS data. Clearly, more validation studies will be required to prove the  
385 ability of the proposed proteins to discriminate between ovarian carcinoma patients and healthy  
386 controls.

387 Although the samples employed in this study were obtained from advanced ovarian cancer  
388 patients and have limited value for the discovery of screening biomarkers, the above validation  
389 data provide the first experimental evidence of the exploitation of the NP protein corona, formed *ex*  
390 *vivo* in human clinical samples, for the discovery of potential biomarker proteins. Considering the  
391 low number of samples used in this study, it should be emphasized that the clinical utility of the  
392 differentially abundant proteins identified as screening or monitoring biomarkers will require  
393 validation in much larger and well-defined patient cohorts and with the appropriate control groups  
394 (i.e. benign gynaecological conditions).

395 Collectively, our results suggest that NPs dispersed in biological fluids have the potential to  
396 be used as an enrichment 'omics' platform for biomarker discovery. It is now well established that  
397 the physicochemical properties of NPs directly affect the composition of protein corona<sup>11</sup> and more  
398 work is needed to investigate whether the use of other types of NPs and/or combinations of  
399 different NPs will further increase the range of plasma proteome detected.

400

401 **Conclusion**

402  
403  
404  
405  
406  
407  
408  
409  
410  
411  
412  
413  
414  
415  
416  
417  
418  
419  
420  
421  
422  
423  
424  
425  
426  
427  
428  
429

In this study, we propose the use of lipid-based nanoparticles as ‘omics’ enrichment platforms to reveal disease specific signatures in the blood of ovarian carcinoma patients. We demonstrate that the molecular composition of protein corona, spontaneously formed around NPs upon incubation with plasma samples, reflects the concentration fluctuations of the blood proteome in the presence of tumorigenesis. Comprehensive comparison between the *ex vivo* formed ‘healthy’ and ‘diseased’ protein coronas by label-free proteomics (LC-MS/MS), revealed the discovery of 413 differentially abundant proteins. Subsequent immunoassay- based validation demonstrated the potential of the nanoparticle-platform proposed to identify novel potential biomarker proteins. This work is thought to pave the way for many more studies needed to allow the clinical exploitation of protein corona fingerprinting as a novel tool to track tumours over time and discover panels of novel biomarkers for early and accurate disease diagnosis.

## 430 **Experimental**

431 **Ethical Approvals.** This project was reviewed and approved by the Manchester Cancer Research Centre  
432 Biobank Sample Access Committee and all sample collection was conducted under the MCRC Biobank  
433 Research Tissue Bank Ethics (ref: 07/H1003/161+5).  
434

435 **Blood sample collection.** Eligible cases for this study included women with recurrent ovarian cancer  
436 commencing Caelyx® chemotherapy as part of standard chemotherapeutic management for disease  
437 progression. Caelyx® contains 2mg/ml doxorubicin hydrochloride encapsulated in a PEGylated liposomal  
438 formulation (16 mg lipid content) and is indicated for the treatment of advanced ovarian cancer in women  
439 who have failed a first-line platinum-based chemotherapy. Plasma samples (before cycle 1 Caelyx® infusion)  
440 were collected into commercially available anticoagulant-treated tubes (K2 EDTA BD Vacutainer®). Plasma  
441 was then prepared by inverting the collection tubes 10 times to ensure mixing of blood with EDTA and  
442 subsequent centrifugation for 12 minutes at 1300 RCF at 4 °C. Following centrifugation supernatant was  
443 immediately collected into labelled Protein LoBind Eppendorf tubes and stored in -80°C. Age-matched  
444 plasma samples from healthy female donors (n=2 Caucasian; n=4 Black; n=4 Hispanic) were purchased from  
445 Seralab UK (LOT BRH1221742-BRH1221751). Considering the impact of the anticoagulant agent on the  
446 formation of the protein corona,<sup>29</sup> healthy plasma samples contained the same anticoagulant agent (K2  
447 EDTA BD Vacutainer® tubes) as that described above for the human clinical samples and were subjected to  
448 the same preparation protocol (centrifugation for 12 min at 1300 rpm at 4 °C). Healthy human plasma  
449 samples were received on dry ice and were stored in a -80°C. Finally, samples were thawed only before the  
450 incubations.  
451

452 **Ex vivo protein corona formation.** To investigate the *ex vivo* protein corona, Caelyx® liposomes were  
453 incubated with plasma samples obtained from recurrent ovarian cancer patients and from healthy donors.  
454 Caelyx® liposomes (20 ul of 0.15 mM) were incubated with 980 ul of plasma for 90 min at 37°C in orbital  
455 shaker at 250 rpm. The *ex vivo* protein corona was allowed to form using the same liposome concentration  
456 (0.15 mM) as that extracted in 1 mL of plasma from intravenously injected patients.<sup>18</sup> This liposome  
457 concentration results in a final sample protein concentration (upon purification of corona-coated liposomes)  
458 that allows in gel digestion of 20ug of protein/sample and subsequent LC-MS/MS analysis. Our previous time  
459 evolution studies of the nanoparticle protein corona demonstrated that a complex protein corona forms as  
460 early as 10 min post-incubation and does not quantitatively change over time.<sup>15</sup> In the present study, we  
461 chose to incubate liposomes for 90 min, which reflects the time of Caelyx® infusion in ovarian carcinoma  
462 patients.  
463

464 **Separation of corona-coated liposomes from unbound and weakly bound proteins.** Corona-coated  
465 liposomes were separated as we have previously described.<sup>15,16</sup> Briefly, *ex vivo* incubated liposomes were  
466 separated from unbound plasma proteins by size exclusion chromatography followed by membrane  
467 ultrafiltration. Immediately after incubation, samples (1ml) were loaded onto a Sepharose CL-4B (Sigma-  
468 Aldrich) column (15cm) equilibrated with HEPES buffer. Fractions containing liposomes (4,5,6) were then  
469 pooled together and concentrated to 500 µL using a Vivaspin 6 column (10 000 MWCO, Sartorius, Fisher  
470 Scientific) at 9000 rpm. Vivaspin 500 centrifugal concentrator (1 000k MWCO, Sartorius, Fisher Scientific)  
471 was then used at 9000 rpm, to further concentrate the samples to 100 µL and to ensure separation of  
472 protein-coated liposomes from the remaining large unbound proteins. Corona-coated liposomes were then  
473 washed 3 times with 100 µL HEPES buffer to remove weakly bound proteins. To validate the separation of  
474 corona-coated liposomes from unbound proteins, the same procedure was performed with controls of plasma  
475 samples (without prior incubation with liposomes (**Figure S1**)).  
476

477 **Transmission Electron Microscopy (TEM).** Bare and corona-coated liposomes were stained by uranyl  
478 acetate solution 1% and visualized with transmission electron microscopy (FEI Tecnai 12 BioTwin) before  
479 and after their *in vivo* interaction with plasma proteins. Samples were diluted to 0.5 mM lipid concentration  
480 and carbon Film Mesh Copper Grids (CF400-Cu, Electron Microscopy Science) were used.  
481

482 **SDS-PAGE electrophoresis.** Proteins associated with 0.025 µM of liposomes were loaded onto a 4-20%  
483 NOVEX Tris-Glycine Protein Gel (ThermoFisher Scientific). The gel was run until the proteins neared the end

484 of the gel (25-40 minutes at 225V). Staining was performed with Imperial Gel Staining reagent (Sigma Life  
485 Science).

486  
487 **Quantification of adsorbed proteins.** Proteins associated with recovered liposomes were quantified by  
488 BCA Protein assay kit according to manufacturer's instructions. To make sure that liposomes in solution do  
489 not interfere with the absorbance at 562 nm we measured the absorbance of corona-coated liposomes in  
490 HEPES buffer and subtracted it from the total absorbance, measured when corona-coated liposomes were  
491 mixed with the BCA reagent. Lipid concentration was quantified by Stewart assay and Protein binding ability;  
492 Pb values ( $\mu\text{g}$  of protein/ $\mu\text{M}$  lipid) were then calculated.

493  
494 **Mass Spectrometry.** In-gel digestion of corona proteins (20 $\mu\text{g}$ /sample) was performed prior to LC-MS/MS  
495 analysis, as we have previously described.<sup>15,16,30</sup> Before SDS-PAGE samples were boiled for 5 min at 90°C  
496 in the presence of Tris-Glycine SDS Sample Buffer and NuPAGE reducing agent (ThermoFisher). Digested  
497 samples were analysed by LC-MS/MS using an UltiMate® 3000 Rapid Separation LC (RSLC, Dionex  
498 Corporation, Sunnyvale, CA) coupled to a Q Exactive™ Hybrid Quadrupole-Orbitrap™ (Thermo Fisher  
499 Scientific, Waltham, MA) mass spectrometer.

500  
501 To assess the repeatability of the sample processing workflow we incubated Caelyx® liposomes with plasma  
502 obtained from a healthy donor and repeated the same protocol for 6 times/replicates (**Figure S2A**). To  
503 assess the analytical variation/repeatability of the LC:MS/MS platform two of the samples used above to  
504 determine the repeatability of the sample processing workflow were run in triplicates (**Figure S2B & S3**). To  
505 assess the linearity of the method we incubated the same concentration of Caelyx® liposomes (0.15 mM) in  
506 full and diluted plasma (**Figure S4**).

507  
508 **Mass Spectrometry data analysis.** To statistically compare the abundance of proteins identified in the  
509 'healthy' and 'diseased' coronas MS peak intensities were analyzed using Progenesis LC-MS software  
510 (version 3.0; Nonlinear Dynamics). RAW files were imported into Progenesis LC-MS software (version 3.0;  
511 Nonlinear Dynamics) with automatic feature detection enabled. The Progenesis QI default method of  
512 normalisation was applied ('Normalise to all proteins') to compensate for experimental variations. A  
513 representative reference run was selected automatically, to which all other runs were aligned in a pair-wise  
514 manner. Automatic processing was selected to run with applied filters for peaks charge state (maximum  
515 charge 5). Protein quantitation method was selected to be the relative quantitation using Hi-N with N=3  
516 peptides to measure per protein. The resulting MS/MS peak lists were exported as a single Mascot generic  
517 file and upload onto a local Mascot Server (version 2.3.0; Matrix Science, UK). The spectra were searched  
518 against the UniProt database using the following parameters: tryptic enzyme digestion with one missed  
519 cleavage allowed, peptide charge of +2 and +3, precursor mass tolerance of 15 mmu, fragment mass  
520 tolerance of 8 ppm, oxidation of methionines as variable modifications and carbamidomethyl as fixed  
521 modifications, with decoy database search disabled and ESI-QUAD-TOF the selected instrument. Each  
522 search produced an XML file from Mascot and the resulted peptides (XML files) were imported back into  
523 Progenesis LC-MS to assign peptides to features. The peptide intensities were compared between groups by  
524 one way analysis of variance. Subsequently data were exported in Excel format. Finally, results were filtered  
525 to present a mean normalized abundance of more than 50,000 in at least one of the two groups.

526  
527 Mass Spectrometry data were also analysed with QIAGEN's Ingenuity® Pathway Analysis (IPA®, QIAGEN  
528 Redwood City, www.qiagen.com/ingenuity). Diseases and functions IPA tool was used to identify proteins  
529 involved in ovarian carcinoma pathways. The biomarker overlay IPA tool was then used to identify proteins  
530 described in the literature as potential biomarkers for ovarian cancer.

531  
532 **Enzyme-linked Immunosorbent Assay (ELISA).** ELISA kits for human CA125 (MUC16, ab195213, Abcam,  
533 UK), apolipoprotein AI (APOAI, ab189576, Abcam, UK), prealbumin (Transthyretin TTR, ab108895, Abcam,  
534 UK), thrombospondin 1 (THBS1, ab193716, Abcam, UK), alpha-enolase (ENO1, ab181417, Abcam, UK),  
535 transforming growth factor beta 1 (TGF- $\beta$ 1, DB100B, R&D Systems Europe, LTD.), nucleoside diphosphate  
536 kinase A (NME1, orb406403, Biorbyt Ltd., UK), glucosidase 2 subunit beta (PRKCSH, EH2259, Wuhan Fine  
537 Biotech Co., Ltd.) and disulphide-isomerase A4 (PDIA4, abx250438, Abbexa Ltd., UK) were purchased for the  
538 quantitative measurement of each human protein in plasma. Experiments were performed according to  
539 manufacturer's instructions

540  
541 **Statistical analysis.** Statistical analysis of the data was performed using GraphPad Prism software. Mann-  
542 Whitney t-test was used for the quantification of the total amount of protein adsorbed (Pb values of **Figure**  
543 **1C**) and for ELISA experiments (**Figure 4B**).  
544

#### 545 **Author contributions**

546 M.H. initiated, designed and performed the experiments, analyzed all data and took responsibility for  
547 planning and writing the manuscript. L.P. contributed to the analysis of the mass spectrometry data. R.U.  
548 provided guidance on the proteomic data analysis. J.R. and A.C. contributed to the clinical design, provided  
549 oversight of the ethical approval process and were responsible for access and storage of the samples in the  
550 MCRC Biobank. K. K. provided intellectual input throughout the study and contributed to the writing of the  
551 manuscript.  
552

#### 553 **Data availability**

554 The raw/processed data required to reproduce these findings are all included in the supporting information.  
555

#### 556 **Acknowledgements**

557 This research was partially funded by the CRUK Pioneer Award (C54921/A25435). We would like to  
558 acknowledge the CRUK/NIHR Manchester Experimental Cancer Medicine Centre for providing research  
559 nurse funding and their clinical infrastructure used for the blood sampling. This work was partially funded by  
560 the CRUK Centre (C147/A18083) and Major Centre Award (C147/A25254) awarded to the Manchester  
561 Cancer Research Centre. We would like to acknowledge the CRUK/NIHR Manchester Experimental Cancer  
562 Medicine Centre for providing research nurse funding and their clinical infrastructure used for the blood  
563 sampling. Authors wish to acknowledge Manchester Cancer Research (MCRC) Biobank team for their  
564 assistance in the collection of blood samples. The authors also would like to thank the Faculty of Life  
565 Sciences EM Facility at the University of Manchester for their assistance in Electron Microscopy imaging. In  
566 addition, Biological Mass Spectrometry (Bio-MS) Facility staff at the University of Manchester for their  
567 support. We would also like to thank the patients for their kind donation of blood samples to support this  
568 research.  
569

570  
571  
572  
573  
574  
575  
576  
577  
578  
579  
580  
581  
582  
583  
584  
585  
586  
587  
588  
589  
590



591  
592  
593  
594  
595  
596  
597  
598  
599  
600  
601  
602  
603  
604  
605  
606  
607  
608  
609  
610  
611  
612  
613  
614  
615  
616  
617  
618  
619  
620  
621  
622  
623  
624  
625  
626  
627  
628  
629  
630  
631  
632  
633  
634  
635  
636  
637  
638  
639  
640  
641  
642  
643  
644  
645

## References

- 1 Fuzery, A. K., Levin, J., Chan, M. M. & Chan, D. W. Translation of proteomic biomarkers into FDA approved cancer diagnostics: issues and challenges. *Clin Proteom* **10**, doi:Artn 13 10.1186/1559-0275-10-13 (2013).
- 2 Anderson, N. L. & Anderson, N. G. The human plasma proteome: history, character, and diagnostic prospects. *Molecular & cellular proteomics : MCP* **1**, 845-867 (2002).
- 3 Hanash, S. M., Pitteri, S. J. & Faca, V. M. Mining the plasma proteome for cancer biomarkers. *Nature* **452**, 571-579, doi:10.1038/nature06916 (2008).
- 4 Rifai, N., Gillette, M. A. & Carr, S. A. Protein biomarker discovery and validation: the long and uncertain path to clinical utility. *Nat biotechnol* **24**, 971-983, doi:10.1038/nbt1235 (2006).
- 5 Liotta, L. A., Ferrari, M. & Petricoin, E. Clinical proteomics: written in blood. *Nature* **425**, 905, doi:10.1038/425905a (2003).
- 6 Tam, J. O. *et al.* A comparison of nanoparticle-antibody conjugation strategies in sandwich immunoassays. *J Immunoassay Immunochem* **38**, 355-377, doi:10.1080/15321819.2016.1269338 (2017).
- 7 Huo, Q. *et al.* A facile nanoparticle immunoassay for cancer biomarker discovery. *J Nanobiotechnology* **9**, 20, doi:10.1186/1477-3155-9-20 (2011).
- 8 Luchini, A. *et al.* Smart hydrogel particles: biomarker harvesting: one-step affinity purification, size exclusion, and protection against degradation. *Nano letters* **8**, 350-361, doi:10.1021/nl072174l (2008).
- 9 Moro, L., Turemis, M., Marini, B., Ippodrino, R. & Giardi, M. T. Better together: Strategies based on magnetic particles and quantum dots for improved biosensing. *Biotechnol Adv* **35**, 51-63, doi:10.1016/j.biotechadv.2016.11.007 (2017).
- 10 Hadjidemetriou, M., Al-Ahmady, Z., Buggio, M., Swift, J. & Kostarelos, K. A novel scavenging tool for cancer biomarker discovery based on the blood-circulating nanoparticle protein corona. *Biomaterials* **188**, 118-129, doi:10.1016/j.biomaterials.2018.10.011 (2019).
- 11 Hadjidemetriou, M. & Kostarelos, K. Nanomedicine: Evolution of the nanoparticle corona. *Nat Nanotechnol* **12**, 288-290, doi:10.1038/nnano.2017.61 (2017).
- 12 Cedervall, T. *et al.* Understanding the nanoparticle-protein corona using methods to quantify exchange rates and affinities of proteins for nanoparticles. *P Natl Acad Sci USA* **104**, 2050-2055, doi:DOI 10.1073/pnas.0608582104 (2007).
- 13 Al-Ahmady, Z. S., Hadjidemetriou, M., Gubbins, J. & Kostarelos, K. Formation of protein corona in vivo affects drug release from temperature-sensitive liposomes. *J Control Release* **276**, 157-167, doi:10.1016/j.jconrel.2018.02.038 (2018).
- 14 Garcia-Alvarez, R., Hadjidemetriou, M., Sanchez-Iglesias, A., Liz-Marzan, L. M. & Kostarelos, K. In vivo formation of protein corona on gold nanoparticles. The effect of their size and shape. *Nanoscale* **10**, 1256-1264, doi:10.1039/c7nr08322j (2018).
- 15 Hadjidemetriou, M., Al-Ahmady, Z. & Kostarelos, K. Time-evolution of in vivo protein corona onto blood-circulating PEGylated liposomal doxorubicin (DOXIL) nanoparticles. *Nanoscale* **8**, 6948-6957, doi:10.1039/c5nr09158f (2016).
- 16 Hadjidemetriou, M. *et al.* In Vivo Biomolecule Corona around Blood-Circulating, Clinically Used and Antibody-Targeted Lipid Bilayer Nanoscale Vesicles. *ACS nano* **9**, 8142-8156, doi:10.1021/acsnano.5b03300 (2015).
- 17 Chen, F. *et al.* Complement proteins bind to nanoparticle protein corona and undergo dynamic exchange in vivo. *Nat Nanotechnol* **12**, 387-393, doi:10.1038/nnano.2016.269 (2017).
- 18 Hadjidemetriou, M. *et al.* The Human In Vivo Biomolecule Corona onto PEGylated Liposomes: A Proof-of-Concept Clinical Study. *Adv Mater*, e1803335, doi:10.1002/adma.201803335 (2018).
- 19 Ke, P. C., Lin, S., Parak, W. J., Davis, T. P. & Caruso, F. A Decade of the Protein Corona. *ACS nano* **11**, 11773-11776, doi:10.1021/acsnano.7b08008 (2017).
- 20 Westmeier, D. *et al.* Nanomaterial-microbe cross-talk: physicochemical principles and (patho)biological consequences. *Chem Soc Rev* **47**, 5312-5337, doi:10.1039/c6cs00691d (2018).
- 21 Miotto, G. *et al.* Protein corona as a proteome fingerprint: The example of hidden biomarkers for cow mastitis. *Colloids Surf B Biointerfaces* **140**, 40-49, doi:10.1016/j.colsurfb.2015.11.043 (2016).

646 22 Magro, M. *et al.* Analysis of hard protein corona composition on selective iron oxide nanoparticles by  
647 MALDI-TOF mass spectrometry: identification and amplification of a hidden mastitis biomarker in  
648 milk proteome. *Anal Bioanal Chem* **410**, 2949-2959, doi:10.1007/s00216-018-0976-z (2018).

649 23 Schiess, R., Wollscheid, B. & Aebersold, R. Targeted proteomic strategy for clinical biomarker  
650 discovery. *Mol Oncol* **3**, 33-44, doi:10.1016/j.molonc.2008.12.001 (2009).

651 24 Nolen, B. M. & Lokshin, A. E. Biomarker testing for ovarian cancer: clinical utility of multiplex assays.  
652 *Mol Diagn Ther* **17**, 139-146, doi:10.1007/s40291-013-0027-6 (2013).

653 25 Office for National Statistics. *Cancer survival by stage at diagnosis for England (experimental  
654 statistics)* , 2016).

655 26 Nolen, B. M. & Lokshin, A. E. Protein biomarkers of ovarian cancer: the forest and the trees. *Future  
656 Oncol* **8**, 55-71, doi:10.2217/fon.11.135 (2012).

657 27 Sandin, M., Chawade, A. & Levander, F. Is label-free LC-MS/MS ready for biomarker discovery?  
658 *Proteomics Clin Appl* **9**, 289-294, doi:10.1002/prca.201400202 (2015).

659 28 Longo, C. *et al.* Core-shell hydrogel particles harvest, concentrate and preserve labile low  
660 abundance biomarkers. *PloS one* **4**, e4763, doi:10.1371/journal.pone.0004763 (2009).

661 29 Schottler, S., Klein, K., Landfester, K. & Mailander, V. Protein source and choice of anticoagulant  
662 decisively affect nanoparticle protein corona and cellular uptake. *Nanoscale* **8**, 5526-5536,  
663 doi:10.1039/c5nr08196c (2016).

664 30 Al-Ahmady, Z. S., Hadjidemetriou, M., Gubbins, J. & Kostarelos, K. Formation of protein corona in  
665 vivo affects drug release from temperature-sensitive liposomes. *Journal of Controlled Release* **276**,  
666 157-167, doi:10.1016/j.jconrel.2018.02.038 (2018).

667  
668  
669  
670  
671  
672  
673  
674  
675  
676  
677  
678  
679  
680  
681  
682  
683  
684  
685  
686  
687  
688  
689

## FIGURE LEGENDS

**Figure 1: Protein corona formation after the *ex vivo* incubation of PEGylated, doxorubicin-encapsulated liposomes (Caelyx<sup>®</sup>) with plasma samples obtained from healthy controls (n=10) and ovarian carcinoma patients (n=19).** (A) Schematic description of the experimental design. Caelyx<sup>®</sup> liposomes were incubated *ex vivo* with plasma samples obtained from patients with recurrent ovarian carcinoma (n=19) and from healthy donors (n=10) for 90 min at 37°C. Corona-coated liposomes were isolated and purified from unbound proteins by size exclusion chromatography and membrane ultrafiltration. ‘Healthy’ and ‘diseased’ protein coronas were comprehensively characterized and compared by label-free mass spectrometry to identify differentially abundant potential biomarker proteins. Selected potential biomarker proteins were further validated by commercially available ELISA kits. (B) Negative stain TEM of liposomes before and after corona formation. All scale bars are 100nm. (C) The total amount of protein adsorbed onto the surface of liposomes recovered from plasma samples obtained from healthy and ovarian carcinoma patients expressed as Pb values ( $\mu\text{g}$  of protein/ $\mu\text{M}$  lipid). Individual biological replicates are shown. Error bars indicate mean  $\pm$  SEM. (Mann-Whitney t-test; \*\*\*\* indicates  $p < 0.0001$ ). (D) Imperial stained SDS-PAGE gel of representative ‘healthy’ and ‘diseased’ corona samples.

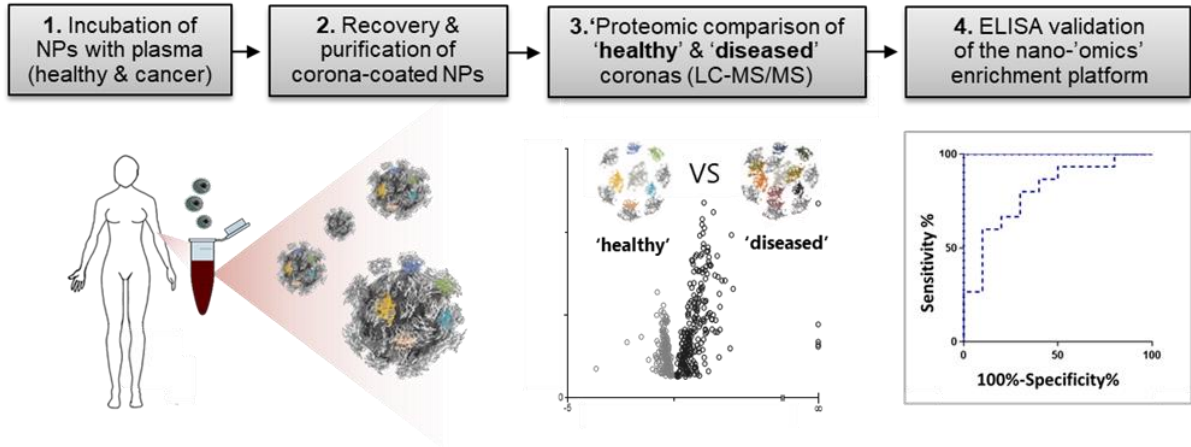
**Figure 2: Proteomic comparison of the liposomal protein coronas formed in plasma samples obtained from ovarian carcinoma patients (n=19) and healthy controls (n=10).** MS peak intensities were analyzed using Progenesis LC-MS software (version 3.0; Nonlinear Dynamics). Results were filtered to present a mean normalized abundance of more than 50,000 in at least one of the two groups. The peptide intensities were compared between groups by one way analysis of variance (ANOVA). (A) Heatmap of Normalized Abundance (NA) values of proteins found to be differentially expressed between ‘healthy’ and ‘diseased’ coronas. Only proteins with  $p$  value  $< 0.05$  are shown (n=413). Proteins are classified from highest to the lowest max fold change. Average abundance of each protein for each group is also shown. The full list of differentially abundant corona proteins and their respective mean normalized abundance,  $p$  value and max fold change are shown in **Table S4**. (B) Volcano plot displays the relationship between fold change and significance between the two groups. The y-axis depicts the negative  $\log_{10}$  of p-values and the x-axis is the difference in expression between the two groups as  $\log_{10}$  fold changes. Only proteins with at least 2-fold change and a  $p$  value  $< 0.01$  value are highlighted (n=303; downregulated proteins are shown in red and upregulated proteins in blue). **Figure 3: Ingenuity Pathway Analysis (IPA) of potential biomarker corona proteins.** Out of 413 potential biomarker proteins n=15 (shown in orange) were previously reported as potential biomarkers for ovarian cancer and n=57 (shown in green) have been previously associated with ovarian carcinoma pathways. The name of proteins illustrated in the diagram and their respective gene symbols are shown in **Table S5**.

**Figure 4: ELISA validation of the nanoparticle protein corona technology.** (A) Scatter plot displays the relationship between fold change and significance of the nine potential biomarker proteins selected to be further validated. The y-axis depicts the negative  $\log_{10}$  of p-values and the x-axis is the difference in expression between the two groups as  $\log_{10}$  fold changes. Clinically used biomarkers are shown in orange, proteins previously associated with ovarian carcinoma pathways (according to IPA) are shown in green and proteins that have not been previously associated with ovarian carcinoma pathways are shown in blue. (B) Plasma concentration profiles of selected potential biomarker proteins in healthy controls (n=10) and ovarian carcinoma patients (n=15-17) and their respective ROC curves based on ELISA assays. AUC values are also shown; Mann-Whitney t-test; \* indicates  $p < 0.05$ , \*\*\* indicates  $p < 0.001$ , \*\*\*\* indicated  $p < 0.0001$ .

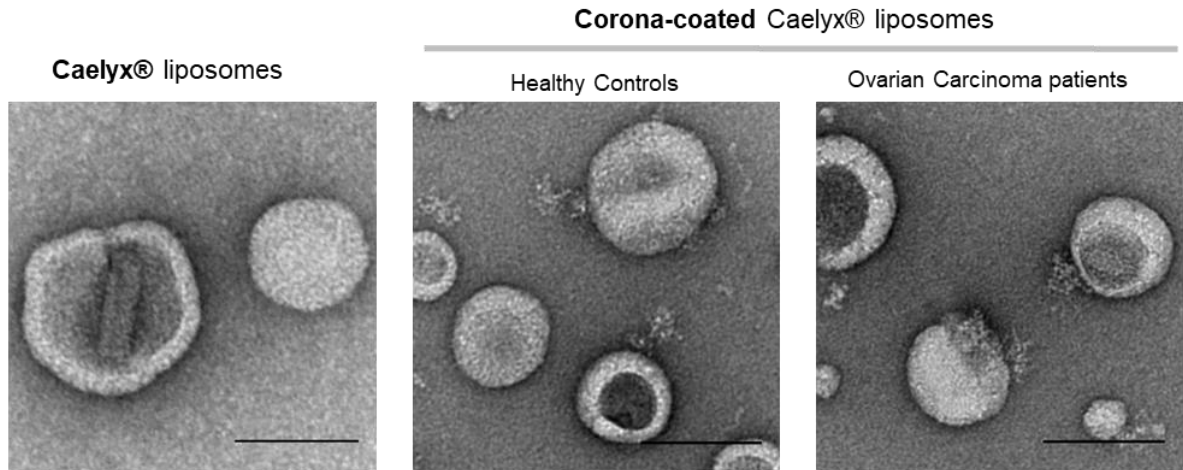
(CA125=mucin 16, APOA1=apolipoprotein A1, TTR=transthyretin, THBS1=thrombospondin 1, ENO1=enolase 1, TGF-b1= transforming growth factor b1, NME1= nucleoside diphosphate kinase A, PRKCSH=glucosidase 2 subunit beta and PDIA4= protein disulfide-isomerase A4).

**FIGURE 1**

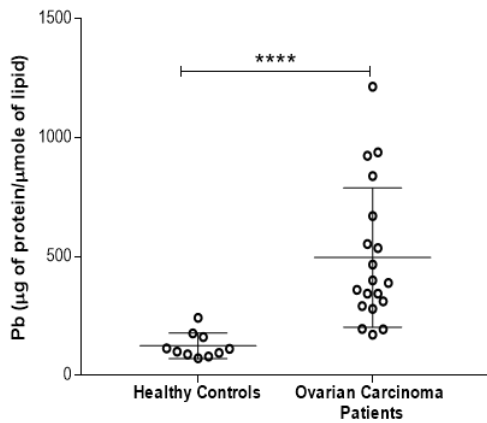
**A**



**B**



**C**



**D**

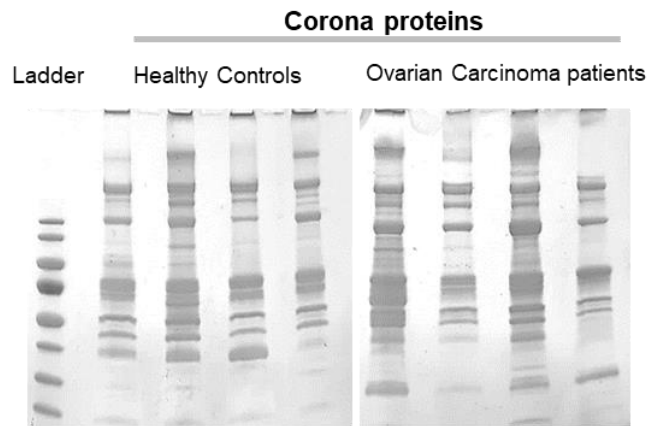
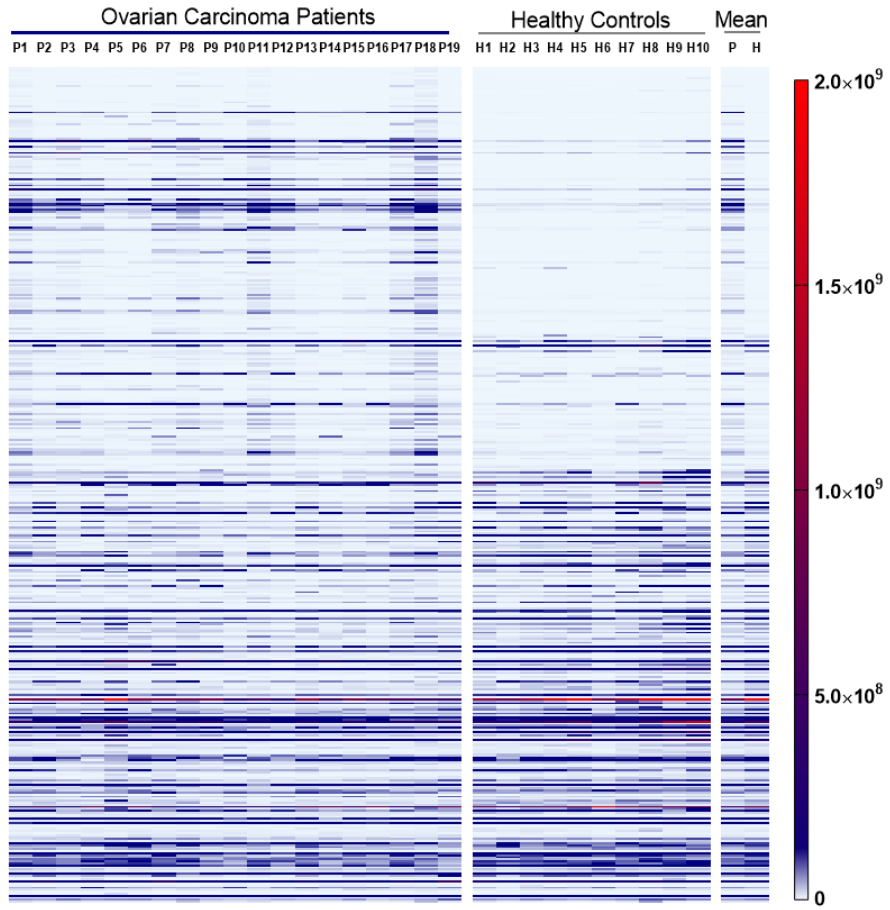
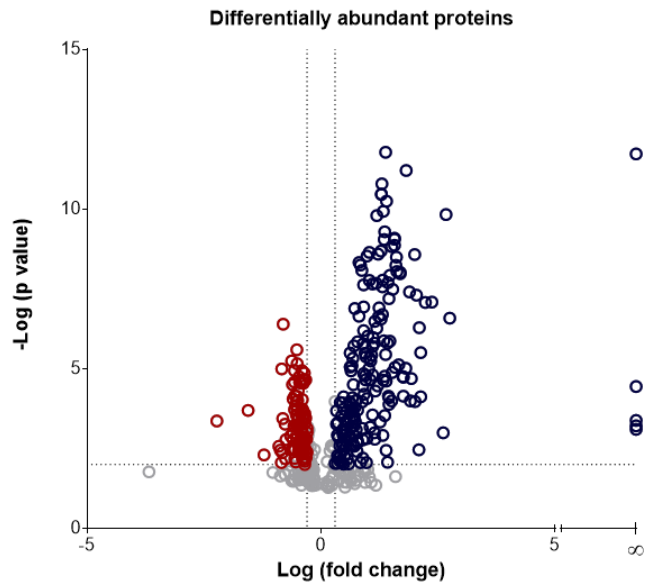


FIGURE 2

**A**

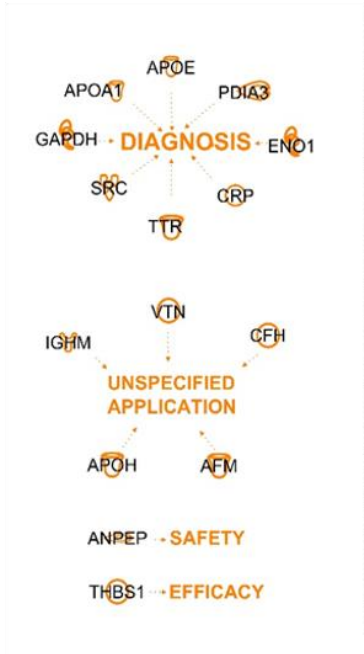


**B**



**FIGURE 3**

Corona proteins previously reported as **potential biomarkers** for ovarian cancer (n=15):



Corona proteins previously reported to be associated with ovarian carcinoma pathways (n=57):

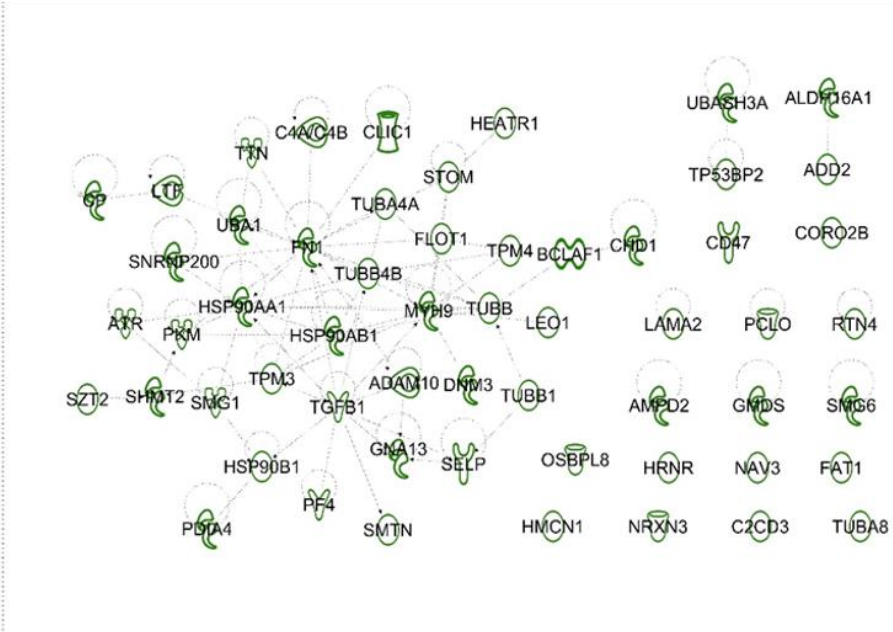
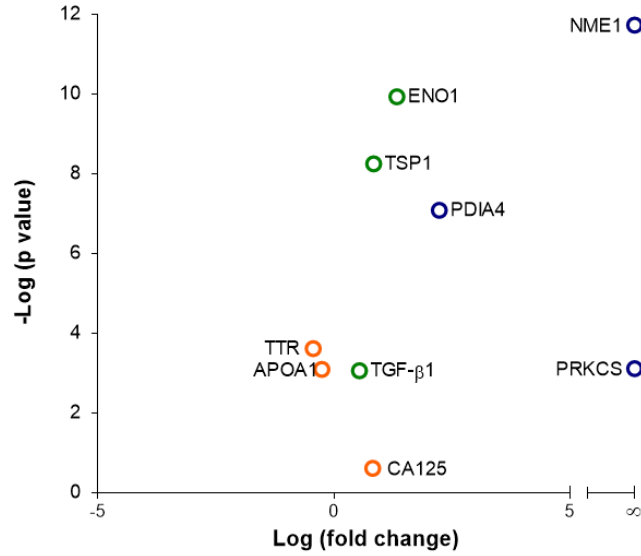


**FIGURE 4**

**A**

Differentially abundant proteins chosen to be validated



**B**

